# FATIGUE CRACK PROPAGATION BEHAVIOR OF ADHESIVELY BONDED CFRP/CFRP AND CFRP/ALUMINUM JOINTS

**Kiyoshi ISHII*, Makoto IMANAKA** , Hideaki NAKAYAMA***
***Osaka Sangyo University, ** Osaka University of Education**
**Key words: Adhesive Joints, Fatigue Crack Propagation, Epoxy adhesive**

***Abstract***

*Fatigue tests were conducted on adhesively bonded CFRP/CFRP and CFRP/aluminum double cantilever beam (DCB) joints to investigate the effect of adherend thickness on the fatigue crack growth rate. Components of joints were unidirectional composite, aluminum plate and a filmy-type epoxy adhesive. The experimental results indicate that the increase of the CFRP or aluminum plate thickness lower the fatigue threshold value and steepens the slope in the Paris region. To elucidate the effect of adherend thickness on the fatigue crack propagation behavior, a finite element analysis conducted to investigate the mode ratio, and stress distributions near the crack tip, where the coefficient of thermal expansion mismatch between the aluminum and the CFRP plates was taken into account. The effect of adherend thickness on the crack propagation rate has been tentatively explained in terms of stress distributions near the crack tip.*

## 1. Introduction

In many CFRP structures, CFRP to CFRP and CFRP to metal adhesively bonded joints are widely used because adhesive bonding has a number of advantages, such as high joint efficiency, no degradation of basic composites, etc. [1]. Hence, it is extremely important to clarify the strength characteristics of these joints, particularly under cyclic loading conditions because many CFRP structures are subjected to cyclic load due to vibration and power transmission. For fatigue studies, adhesively bonded double cantilever beam (DCB) joints has been most commonly used, in which the effect of bond line thickness, loading frequency and mix mode loading on fatigue crack propagation has been well investigated [2-6]. However, little information exits on the influence of adherend thickness [7].

In this study, the effect of adherend thickness on the fatigue propagation rate was investigated by using adhesively bonded CFRP/CFRP and CFRP/aluminum DCB joints. Experimental results were discussed from the view point of stress distributions near the crack tip obtained by a finite element analysis and the observation of fracture surfaces.

| Joint type | Plate thickness |
|---|---|
| CFRP/CFRP DCB joint | $t_1=t_2=2,3,4$mm |
| CFRP/aluminum DCB joint | $t_1$(aluminum)=2.6mm, 10mm<br>$t_2$(CFRP)=3mm |

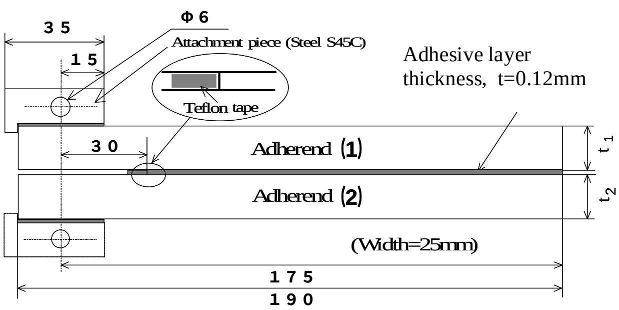


Fig. 1 Shape and dimensions of the adhesively bonded DCB joint.

## 2. Experimental procedure

Figure 1 shows shape and dimensions of the adhesively bonded DCB joints used for the fatigue test. Adherends were used aluminum alloy (JIS 2017-T4) and a unidirectional CFRP composite whose carbon fiber and matrix epoxy resin were Mitsubishi Rayon, TR50S and #350, respectively. And a film-type epoxy adhesive (Mitsubishi Rayon NB101 HC50) was used. Two types of joints were

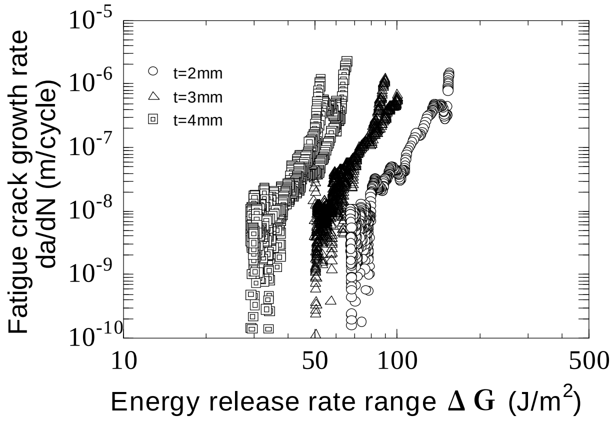


Fig.2 Fatigue crack propagation curves for CFRP/CFRP joints.

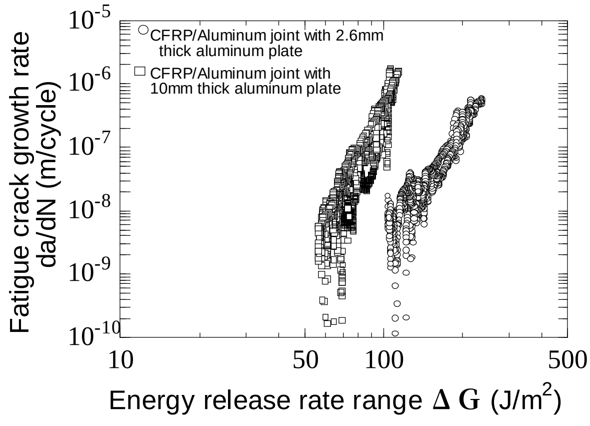


Fig.3 Fatigue crack propagation curves for CFRP/aluminum joints.

fabricated: one is symmetric CFRP/CFRP joints, another is asymmetric CFRP/aluminum joints. The adhesively bonded DCB joints were prepared as follows. The bonding surfaces of adherends were polished with an emery paper of grade 120 mesh under dry conditions. Then, the adhereds were degreased with acetone in an ultrasonic bath. These joints were cured at 303K for 1 hr, cooled in a furnace.

Fatigue tests were carried out under displacement control condition with a displacement ratio $R(\delta_{min}/\delta_{max})$ = 0.2 and loading frequency of f=2Hz. To generate the initial fatigue crack from pre-cracked induced by a Teflon tape as in Fig.1, the joints were applied to cyclical loading. Then fatigue crack growth test was conducted to measure the crack growth rate. To monitor the crack length, *a* and the strain energy release rate, *G* in the fatigue process, the applied load, *P* and the displacement between the loading points, $\delta$ were recorded at suitable intervals. For both the adhesively-bonded CFRP/CFRP and CFRP/aluminum DCB joints, linear relationship between the crack length, *a* and the cube root of the compliance, $C^{1/3}$ was observed as shown in equation (1),

$$C^{1/3} = pa + q, \qquad (1)$$

where *p* and *q* are regression coefficients. In this fatigue tests, measured crack length using a traveling microscope agreed well with the calculated one using Eq. (1). Thus the crack length was determined using the unloading compliance method.

The strain energy release rate is calculated by the following equation:

$$G = \frac{P^2}{2B}\frac{dC}{da}, \qquad (2)$$

Where *P* is the applied load, *B* is the width of the joint, *a* is crack length and *C* is compliance. *dC/da* was calculated from Eq.(1).

## 3 Experimental results

### 3.1 Fatigue crack propagation tests

Figures 2 and 3 show the fatigue crack growth rate, *da/dN* against the range of energy release rate, $\Delta G = G_{max} - G_{min}$, for the CFRP/CFRP and CFRP/aluminum DCB joints. For both the joints, plots of *da/dn* against $\Delta G$ consist of regions Ⅰ and Ⅱ. The former region is associated with a fatigue threshold, and for the latter one the Paris relationship. As shown in Fig.2 and 3, the increase of the plate thickness raises the slope of curve in region Ⅱ and decreases the fatigue threshold value for the both joints. Mangalgi et al had also observed that the slope in region Ⅱ is also increases with the increase CFRP plate thickness for both symmetric and asymmetric CFRP/CFRP joints [7]. However, in the region Ⅰ their results indicated that $\Delta G$ at $10^{-9}$m/cycle which is nearly equal to the fatigue threshold decreased with the decrease in the plate thickness for both symmetric and asymmetric joints, which is different from the results for the present joints. On the other hand, the effect of the thickness of adherend on fracture toughness for adhesively bonded DCB joints have been investigated under static load condition, wherein it was confirmed that fracture toughness increased with the increase in flexural rigidity of the adherend [8,9]. The above trend is similar to that for the present fatigue tests. In the present situation, the effect of adherend thickness on fatigue or fracture toughness has been still unclear.

### 3.2 Observation of fracture surfaces

Figure 4 and 5 show fracture surfaces for the CFRP/CFRP and CFRP/aluminum specimens, respectively, where some parts of the fracture surfaces for the both joints are observed by a laser microscope. Besides, to maintain the adhesive layer thickness, the adhesive contains some fibers whose diameter is about 50 μm. A Laser microscopic image for the CFRP/CFRP specimen indicates that the fibers to maintain the thickness are rarely observed as in Fig.4, whereas the fibers are observed in fracture surface for the CFRP/aluminum joint as in Fig.5 (a) and (b). It is expected from the observation that the crack for the CFRP/CFRP joint mainly propagates near the interface and the crack propagates near the middle part in the adhesive layer for the CFRP/aluminum joint. The macroscopic view for the CFRP/CFRP joint shows rough surface, where some nail marks are observed. On the other hand, fracture patter for the CFRP/aluminum joints varies with the thickness of aluminum plate. For the CFRP/aluminum joint with 2.6mm thick aluminum plate the fracture surface is relatively flat , whereas that for the joint with a 10mm thick aluminum plate indicates rough surface similar to the CFRP/CFRP joint, where same nail marks are accompanied by some trace of carbon fibers as in Fig.5(b).

## 4. Finite Element Analysis

To investigate the relation between the crack propagation rate and stress distribution near the crack tip for the both joints, finite element analysis was carried out using the finite element code MSC-Marc, for which four-node plane strain element was used. In this analysis, residual thermal stress during cool-down process form curing temperature has been taken into account, because thermal expansion coefficient in epoxy adhesive or aluminum plate is over ten times greater than that in CFRP plate. In this analysis, the aluminum and CFRP plates are treated as elastic materials. To obtain maretial constants of the adhesive, a torsional test has been conducted by using adhesively bonded tubular butt joints. Figure 7 shows the shear stress-strain curve for the tubular butt joint. It is reasonable to assume the adhesive as an elastic-perfectly plastic material

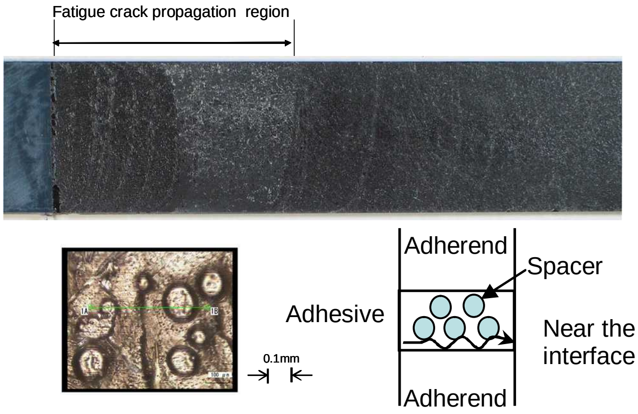


Fig.4 Fracture surfaces of CFRP/CFRP joint with 2mm thick CFRP plate.

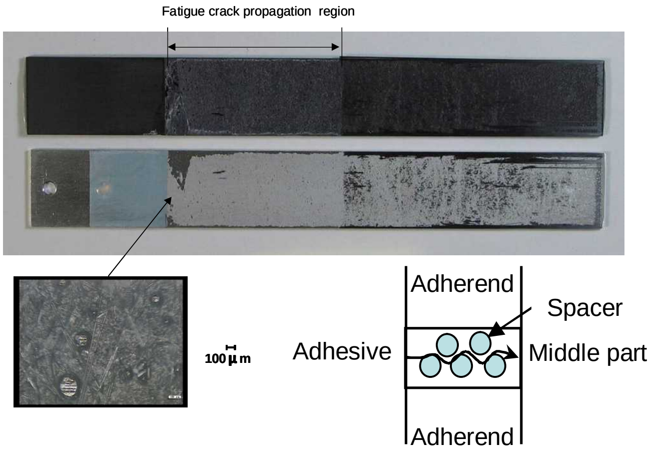


(a)2.6mm thick aluminum plate

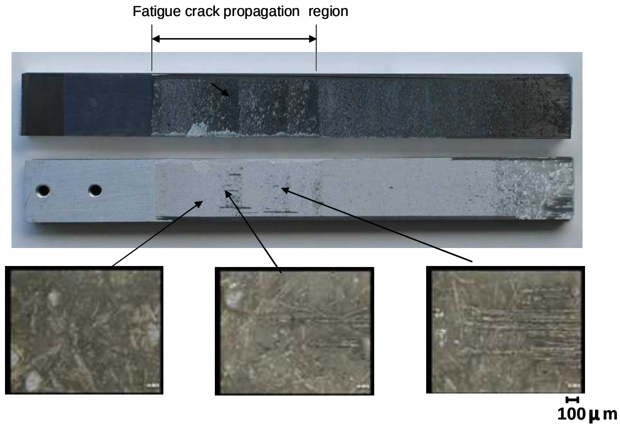


(b) 10mm thick aluminum plate

Fig.5 Fracture surfaces of CFRP/aluminum joints.

from the shape of the curve as in Fig.6. Material constants used for the analysis are shown in Table 1.

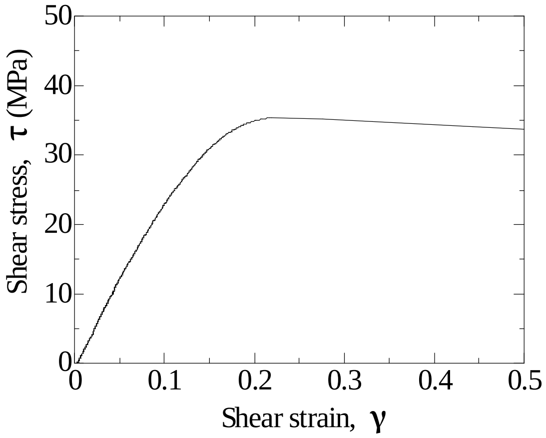


Fig.6 Shear stress-strain curve for the adhesive.

Table 1 Material constants for the analysis.

| Material | Moduli of elasticity (GPa) | Poisson's ratio | Yield stress (GPa) | Coefficient of thermal expansion (/K) |
|---|---|---|---|---|
| CFRP | $E_{xx}$=130.0, $G_{xy}$=6.266<br>$E_{yy}$=10.49, $G_{yz}$=4.297<br>$E_{zz}$=10.49, $G_{zx}$=6.266 | $\nu_{xy}$=0.280<br>$\nu_{yz}$=0.226<br>$\nu_{zx}$=0.022 | | $1.00\times10^{-6}$ |
| Aluminum plate | E=75.4 | $\nu$=0.34 | | $2.36\times10^{-5}$ |
| Adhesive | E=3.88 | $\nu$=0.29 | $\sigma_y$=59.4 | $3.00\times10^{-5}$ |

### 4.1 Thermal stress during the cool-down process from curing temperature

Due to the difference in the thermal expansion coefficient between CFRP and aluminum plates, an adhesively bonded CFRP/aluminum DCB joint were bent during the cool-down from the curing temperature, as shown in Fig.8. This means that the residual stress was generated in the adhesive layer. The residual stress depends on $\Delta T = T_0 - T_{SF}$, where $T_0$ and $T_{SF}$ are the room and stress free temperatures, respectively. Material constants of adhesive layer vary with temperature. Simultaneously, a bulk shrinkage also occurs curing process. Hence, a theoretical analysis of the residual stress is very difficult. Here, to evaluate the residual stress, deformation of the CFRP/aluminum joint with a 2.6mm thick aluminum plate was simulated using the apparent temperature drop, the material constants were assumed to be constant during the cooling process. The calculated deflection with $\Delta T$=-35K was 3.528mm, which is nearly equal to the experimentally obtained value of $\delta_{max}$ =3.5mm. Hereafter, this apparent temperature drop was used


Fig.7 Deformation of the CFRP/aluminum DCB joint with 2.6mm thick aluminum plate during cool down process.

to evaluate the thermal stress generated during the cool-down process.

### 4.2 Stress distributions

#### 4.2.1 CFRP/CFRP DCB joint

The fracture surface for the CFRP/CFRP joint indicates that crack propagates near the adhesive/adherend interface. According to the observation, a crack tip has been located at the adhesive/CFRP interface in this analysis. Figure 8 shows the maximum principal stress distributions in front of the crack tip, where the energy release rate for the joints are fixed to 80J/m$^2$. As shown in this figure, the stress distribution with 2mm thick is nearly equal to that with 3mm thick, whereas the stress distribution with 4mm thick is a little greater than that with 2 or 3mm thick. Generally, the increase of the stress promotes the evolution of damage near the crack tip, which raises the fatigue crack growth rate. According to the general

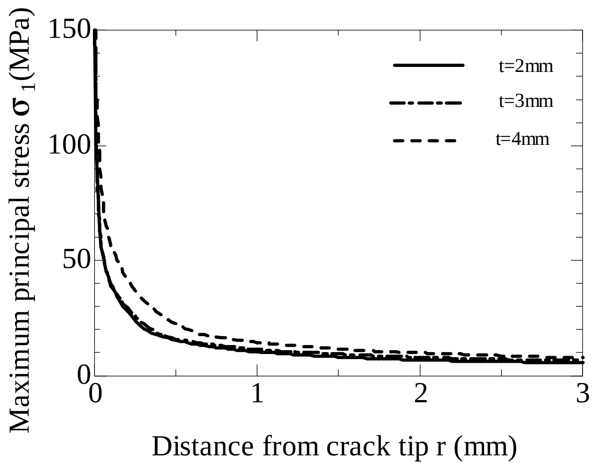


Fig.8 The maximum principal stress distributions for the CFRP/CFRP joints ($G$=80J/m$^2$).

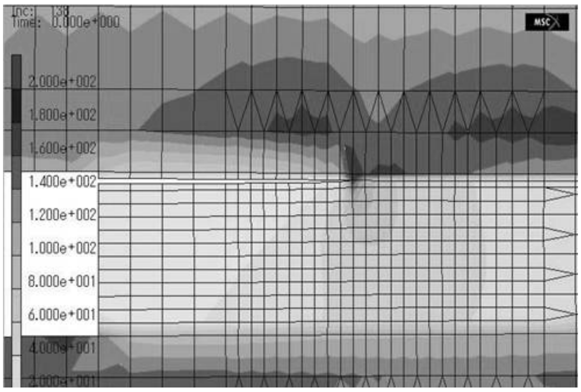

(a) 2mm thick CFRP plate

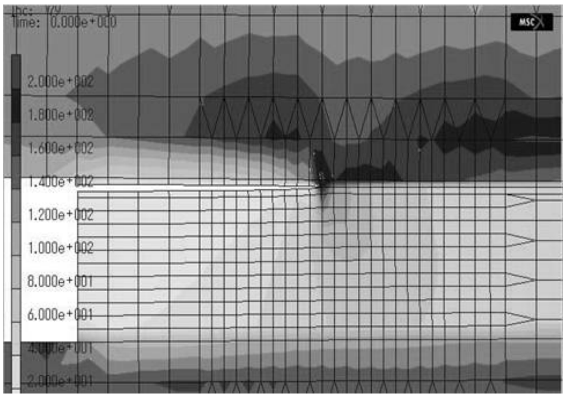

(b) 4mm thick CFRP plate

Fig.9 Contour plots of the maximum principal stress near the crack tip for the CFRP/CFRP joints($G$=80J/$m^2$).

tendency as above, the fatigue crack growth rate for the CFRP/CFRP joints increases with increasing the maximum principal stress. However, the effect of the plate thickness on the maximum principal stress distribution is small in front of the crack tip.

To search other causes, effect of the plate thickness on the stress distribution in the adherend has been investigated. Figure 9 (a) and (b) shows the contour plots near the crack tip for the CFRP/CFRP joints with 2mm and 4 mm thick CFRP plates, respectively. As shown in Fig.9, high stress concentrated zone appears in the CFRP plate near the interface for the both joints. Beside, the matrix of the CFRP is an epoxy resin whose strength dose not so differ from that of the adhesive. Hence, the high concentrated stress may generate the damage of the CFRP plate, which may increase the fatigue crack growth rate for CFRP/CFRP joints. This figure also indicates that stress level for the joint with 4mm thick is higher than that for the joint with 2mm thick,

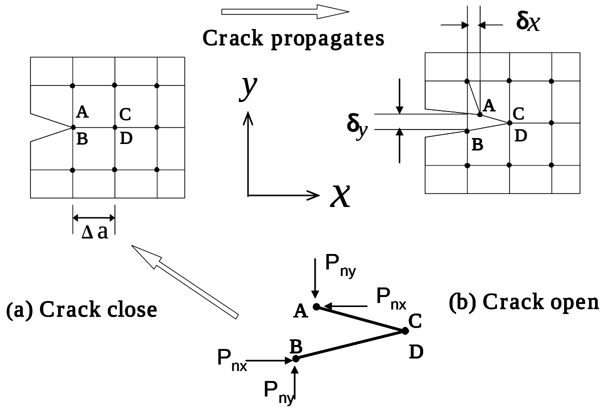


Fig.10 Modified crack closure technique.

and the high stress area expands with the increase of plate thickness. This may be one reason why the crack propagation rate for the CFRP joint increase with the increase of the plate thickness.

### 4.2.1 CFRP/aluminum DCB joint

For the CFRP/aluminum joint, the mode ratio, $G_{II}/G_{I}$, at the crack tip varies with crack length due to asymmetrical combination of the adherends. To obtain the mode ratio, modes I and II strain energy release rates are calculated by a modified crack closure technique [10]. Figure 10 shows schematic illustration of the technique, where a very stiff spring element is located between Nodes C and D. Figures 10(a) and (b) indicate a mesh pattern before and after crack propagation, $P_{nx}$ and $P_{ny}$ indicate crack closing forces in the x and y directions which are required to return the Nodes A and B to their original points, $\delta_x$ and $\delta_y$ are x and y directional relative displacements between Nodes A and B. The nodal force multiplied by the nodal displacement is the amount of work required to close the crack tip. Hence, the strain energy release rate is given by dividing the work by the amount of new crack area formed when the crack propagates. Thus, Modes I and II strain energy release rates are given as follows:

$$G_{\mathrm{I}} = \frac{\delta_y P_{ny}}{2\Delta a} \qquad G_{\mathrm{II}} = \frac{\delta_x P_{nx}}{2\Delta a} \tag{4}$$

Figure 11 shows the mode ratio, $G_{II}/G_{I}$ as a function of crack length under the condition that displacement between the loading points has a constant value of 3 mm. As shown in Fig.11,

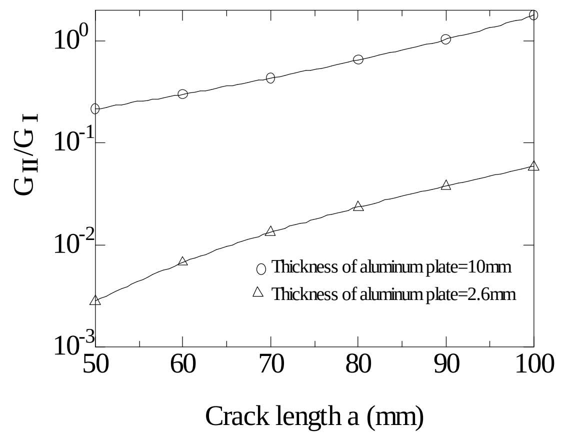


Fig.11 The mode ratio $G_{II}/G_{I}$ as a function of crack length.

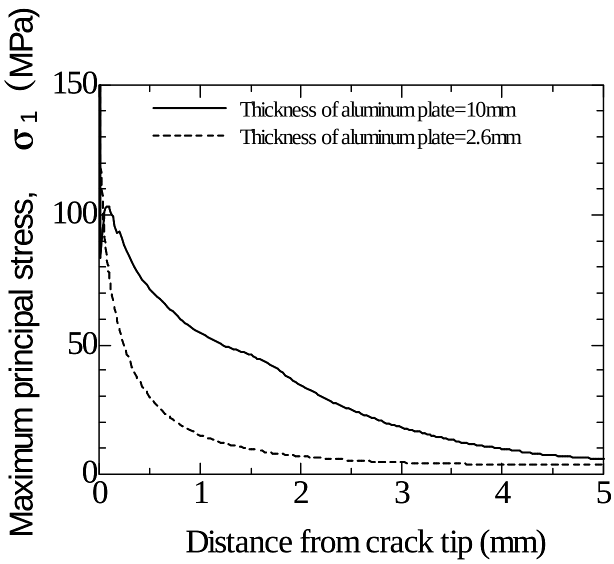


Fig.12 The maximum principal stress distribution for the CFRP/aluminum joints($G$=150J/m$^2$).

$G_{II}/G_{I}$ increases with the increase in crack length for both joints. As the displacement is constant in this analysis, the increase in the crack length corresponds to the decrease in the applied load. A similar trend with the portion of mode II increasing with decreasing applied load was confirmed for the boron-epoxy/aluminum DCB joint. This is explained in terms of the residual stress, i.e. $G_{II}$ still exists at zero load due to residual stress, whereas $G_{I}$ does not [11]. This figure also indicates that $G_{II}/G_{I}$ for the joint with a 10mm thick aluminum plate is over ten times greater than that for the joint with a 2.6mm thick one.

The ratio, $G_{II}/G_{I}$ is related to the direction of crack extension. With an increase in the mode ratio, the direction of the fatigue crack deviates to the adhesive layer and turn to the CFRP plate. As shown in Fig.5(b), fracture surfaces for the joint with 10mm thick aluminum plate indicate that trace of fibers increased with increasing crack length. These observations agree with the results of Fig.11, because the ratio, $G_{II}/G_{I}$ increases with the crack length.

Similar to the CFRP/CFRP joints, the maximum principal stress distributions for the CFRP/aluminum joints near the crack tip are shown in Fig.12, where the energy release rate for the joint are fixed to 150J/m$^2$. As above mentioned, the crack for the CFRP/aluminum joints tends to turn to the CFRP plate, and trace of fibers observed. However, in many parts of fracture surfaces crack propagates in the middle part of the adhesive layer. In this analysis, the crack is located in the middle of the adhesive layer. As shown in this figure, the stress value in the vicinity of the crack tip for the joint of 10mm thick aluminum plate is nearly equal to that of 2.6mm thick. However, the stress in the joint with 10 mm thick is higher over a long range than that in the joint of 2.6mm thickness. Similar to the CFRP/CFRP joint, the fatigue crack growth rate for the CFRP/aluminum joints increases with increasing the maximum principal stress. Though the difference of the stress distributions is considerably greater than the difference of the stress distributions between CFRP/CFRP joint with 2mm thick and that with 4mm thick, the difference of the fatigue threshold values for the CFRP/aluminium joints is close to that for CFRP/CFRP joints. Generally, the fatigue crack propagation rate decreases with increasing the mode ratio, $G_{II}/G_{I}$. As above mentioned the mode ratio for the CFRP/aluminum joint with 2.6mm thick is nearly equal to zero. On the other hand, the mode II component for the joint with 10mm thick can not be negligible, which may decrease the fatigue crack propagation rate. This may be one reason why the difference of he fatigue threshold values for CFRP/aluminium joints is close to the difference for the CFRP/CFRP joints.

The stress distributions in the adherend have been also investigated. Figure 13 (a) and (b) shows the contour plots near the crack tip for the CFRP/aluminum joints with 2mm and 10mm thick aluminum plates, respectively. Similar to the CFRP/CFRP joints as in Fig.9, high stress concentrated zone appears in the CFRP plate near the interface for the both joints, and the stress level for the joint with 10mm thick is higher than that for the joint with 2.6mm thick, and high stress area also expands with the increase in the plate thickness.

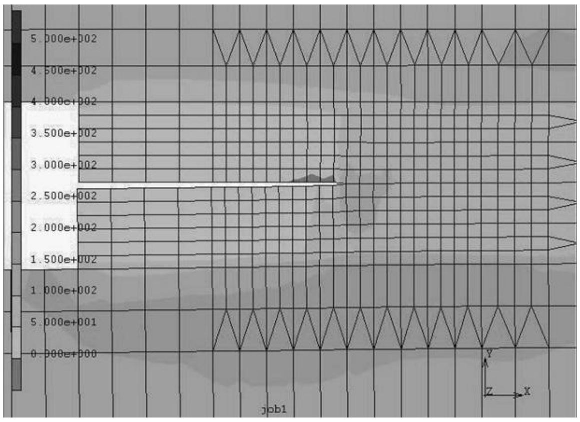


(a) 2.6mm thick aluminum plate

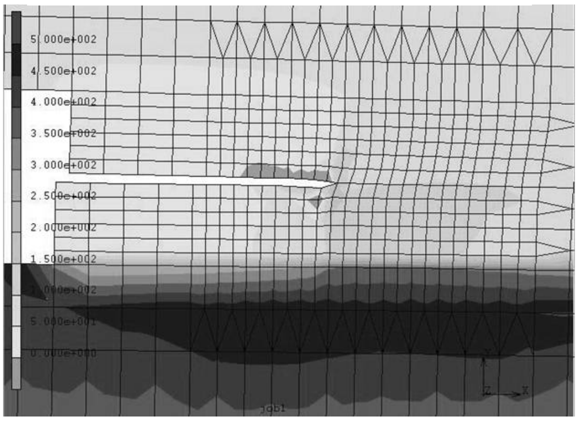


(b) 10mm thick aluminum plate

Fig.13 Contour plots of the maximum principal stress near the crack tip for the CFRP/aluminum joints ($G=150J/m^2$).

## 5. Conclusions

Fatigue tests were conducted on adhesively bonded CFRP/CFRP and CFRP/aluminum DCB joints to investigate the effect of adherend thickness on the fatigue crack growth rate. To clarify the experimental results regarding the mode ratio and stress distribution near the crack tip, a finite element analysis was also conducted. The main results obtained are as follows.

1. The increase in the plate thickness lowers the fatigue threshold value and steepens the slope in the Paris region for the both CFRP/CFRP and CFRP/Aluminum joints,
2. The crack mainly propagates near the interface and a rough fracture surface is observed for the CFRP/CFRP joints. On the other hand, for CFRP/aluminum joints, cracks propagated in the middle part of the adhesive layer irrespective of the aluminum plate thickness. Fracture surface for the joint with 2.6mm thick aluminum plate is smooth, whereas the surface is rough and trace of the carbon fibers appears in some parts for the joint with 10mm thick aluminum plate.
3. The maximum principal stress in front of the crack tip increases with the increase in the plate thickness for the both CFRP/CFRP and CFRP/Aluminum joints, wherein the effect of the plate thickness on the maximum principal stress for the CFRP/CFRP joints is smaller than that for the CFRP/aluminum joints.
4. High stress concentrated zone appears in the CFRP plate near the interface for the both CFRP/CFRP and CFRP/aluminum joints. The stress level and extent of the high stress area increase with the increase in the plate thickness for the both joints.
5. Mode II energy release rate is negligible small for the CFRP/aluminum joint with 2.6mm thick aluminum plate, whereas the mode ratio, $G_{II}/G_I$ for the joint with a 10mm thick aluminum plate is over ten times greater than that for the joint with 2.6mm thick one, and the mode ratio increases with the crack length for both joints.

**Acknowledgements**

The authors acknowledge the provision of CFRP plates and adhesive from Mitsubishi Rayon Co.Ltd.

## References

[1] Adams R.D.and Wake W. " *Structural Adhesive Joints in Engineering"*, Elsevier, 1984.

[2] Ashcroft I.A. and Shaw S.J. "Mode I fracture of epoxy bonded composite joints:2.Fatigue loading", *Int. J. Adhesion Adhesives"*, Vol.22, pp 151-167, 2002.

[3] Erpolat S., Ashcroft I.A., Crocombe A.D. and Wahab M.A. "On the analytical determination of strain energy release rate in bonded DCB joints", E*ng. Fracture Mech.***,** Vol.71, pp.1393-1401,2004.

[4]Abdel M.M., Ashcroft I.A. and Smith P.A. "Finite element prediction of fatigue crack propagation lifetime in composite bonded joints" *Composites*, *Part A*, Vol.35, pp 213-222, 2004.

[5] Mall S. and Yun K.T. "Effect of adhesive ductility on cyclic debond mechanism in composite-to-composite bonded joints", *J. Adhesion*, Vol.23, pp 215-231, 1987.

[6] Mall S., Rezaizadeh M.A. and Gurumurthy R. "Interaction of mixed mode loading on cyclic debonding in adhesively bonded composite joints", *J. Eng. Mater. Technol.*, Vol.109, pp 17-21, 1987.

[7] Mangalgi P.D., Johnson W.S. and Everett R.A Jr. "Effect of adherend thickness and mix mode loading on debond growth in adhesively bonded composite joints", *J.Adhesion*, Vol.23, pp 63-288, 1987.

[8] Bell A.J. and Kinloch A.J. "Effect of the substrate material on the value of the adhesive fracture energy, $G_c$", J. Marer. Sci. Lett. Vol.16, pp 1450-1253, 1997.

[9] Yan C., Mai Y.-W. and Yuan Q. , Ye Q. and Sun J. "Effect of the substrate materials on fracture toughness measurement in adhesive joints", Int. J. Mat. Sci., Vol.43

[10] Rybicki E.F., and Kanninen M.F. "A finite element calculation of stress intensity factors by a modified crack closure integral", *Eng. Fracture Mech.*, Vol.9, pp 931-938, 1977.

[11] Valentin R.V., Butkus L.M. and Johnson W.S. "A finite element and experimental evaluation of boron-epoxy doublers bonded to aluminum substrate" *J. Composite Technol. Res.*,Vol. 20, pp 108-119,1998.